INTERNATIONAL JOURNAL FOR NUMERICAL AND ANALYTICAL METHODS IN GEOMECHANICS
Int. J. Numer. Anal. Meth. Geomech., **23**, 1521–1534 (1999)

A HYBRID FINITE ELEMENT METHOD FOR FLUID-FILLED POROUS MATERIALS

DAN ZENG[1], NORIKO KATSUBE AND JINMIAO ZHANG[2]

[1] *Boyd Laboratory, Department of Aerospace Engineering, Applied Mechanics, and Aviation, The Ohio State University, 155 W. Woodruff Ave., Columbus, Ohio 43210, U.S.A.*
[2] *Battelle Memorial Institute, 505 King Avenue, Columbus, Ohio 43201, U.S.A.*

SUMMARY

A hybrid finite element method is proposed for the thermo-mechanical analysis of porous materials with pore pressure. Arbitrary *n*-sided polygonal elements based on the Hellinger–Reissner principle are used to mesh the heterogeneous domain. The validity of the proposed method is verified by a simple analytical solution and the results obtained by the conventional finite element method (ABAQUS). Irregular local stress distribution on a porous material with randomly distributed holes is predicted by the proposed method. Copyright © 1999 John Wiley & Sons, Ltd.

KEY WORDS: hybrid finite element method; porous materials; randomly distributed pores

1. INTRODUCTION

Thermo-mechanical response of fluid-filled porous materials has wide applications in geotechnical engineering, material science and engineering, and various manufacturing processes. While the overall material properties have been examined through the volume-average methods[1,2], the effect of the random distribution of pores and pore pressure on the local material behaviour has not been well established. Since the initiation of material degradation and failure is determined by the microstructure of the material, the knowledge at the micro-level is important.

In problems of fluid-filled porous materials, the deformation of a porous material and the flow of a fluid through a porous material are normally coupled through the equations of equilibrium, Darcy's law, continuity, and constitutive relations. In steady-state problems, however, the problems can be uncoupled, and the fluid pressure can be evaluated from the fluid mass continuity equations and Darcy's law. In this work, we will focus our attention on this class of uncoupled problems and develop a finite element method for a fluid-filled porous material where circular holes are randomly distributed and each pore is subjected to specified pore pressure. This work is the further development of the recently developed hybrid method by Zhang and Katsube[3–5] for fluid-filled porous materials.

* Correspondence to: N. Katsube, Boyd Laboratory, Department of Aerospace Engineering, Applied Mechanics, and Aviation, The Ohio State University, 155 W. Woodruff Ave., Columbus, Ohio 43210, U.S.A.

Contract grant sponsor: National Science Foundation; contract grant number: CMS9634870.

CCC 0363–9061/99/131521–14$17.50

Received 21 January 1998
Revised 31 August 1998

Finite element analysis of porous materials requires the generation of complicated meshes due to the random distribution of the pores. It is therefore often difficult to generate finite element meshes especially when the number of the pores is large. Ghosh and his co-workers[6,7] have applied the notion of the Voronoi cell to heterogeneous problems with a random distribution. An n-sided polygon includes an inclusion (pore) and serves as an element. The complexity of generating a conventional mesh is thus avoided. This notion has been employed in References 3–5, 8 and it will be again employed in this work.

In developing super elements, the present work closely follows the hybrid methods pioneered by Tong *et al.*[9] and also by Piltner[10]. Tong *et al.*[9] developed the hybrid methods for a crack based on the Hellinger–Reissner principle. Piltner[10] also employed the hybrid method in developing special elements for holes and internal cracks. Following their work[9,10], Zhang and Katsube[3–5] and Zhang[8] applied their notion to heterogeneous materials with randomly distributed inclusions.

In all these works[3–5,8–10], the classical elasticity solutions are directly used to approximate both stress and displacement fields as shape functions inside the super elements. Since the trial functions themselves reflect actual stress and displacement distributions around the pores, cracks, or inclusions, the developed methods have been proven to be extremely accurate and efficient.

Even though the same circular/elliptical inclusion problems are addressed, there are minor differences in terms of shape functions between the work by Piltner[10] and that by Zhang and Katsube[3–5]. The shape functions used by Piltner[10] automatically satisfy the internal boundary condition, while those used by Zhang and Katsube[3–5] remain general.

In this work, a special super element for a fluid-filled porous material will be developed. The hybrid functional for the mixed boundary conditions in Reference 8 is used in a super element where a circular pore is included and subjected to a constant hydrostatic pressure. Since the shape functions used in References 3, 4 are for a circular hole with any internal boundary condition, the same shape functions are employed here. Due to the specified hydrostatic pore pressure, the load vector is required for the special element. The stationary value of the hybrid functional leads to the derivation of the appropriate element stiffness matrix and the load vector.

The accuracy of the newly developed super element has been verified by comparing our results with the analytical solution of stress distribution in an infinite (large) plate containing a single circular hole subjected to hydrostatic pressure. In a boundary value problem with four regularly spaced pores, 196 coarse hybrid elements are used to obtain results that are comparable to those predicted by using a complex mesh with 8832 conventional elements. The developed method is applied to a boundary value problem where fluid pressure is determined from Darcy's law and the continuity equation. The effects of random pore distribution and pore pressure on local stress concentrations are numerically evaluated.

The problems of fluid-filled porous materials and those of thermo-mechanical theory for porous materials share similar theoretical structures. Based on this similarity, the proposed method can be easily applied to calculate thermal residual stresses of porous materials. A boundary value problem demonstrating this fact is shown as an example.

2. BASIC FORMULATIONS

Figure 1 shows an n-sided polygonal special element **e** where a hole is embedded and is subjected to a uniform hydrostatic pressure on the internal boundary. The domain, the outer and inner boundary of the element are, respectively, represented by Ω, c_1 and c_2.

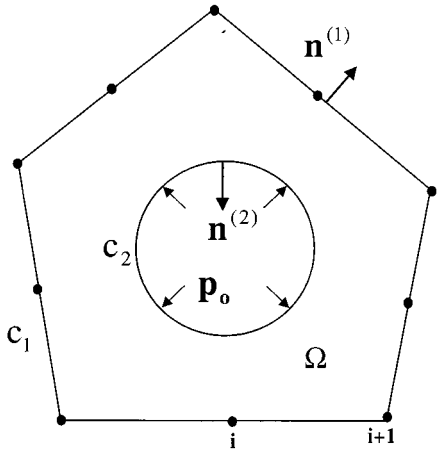

Figure 1. An n-sided polygonal special element

Following the Hellinger–Reissner principle, the hybrid functional over the element **e** as in Reference 8 is employed

$$\Pi_e = \frac{1}{2}\int_\Omega [\sigma \mathbf{S}\sigma - \sigma(\mathbf{D}\mathbf{u})]\,\mathrm{d}\Omega - \oint_{c_1} \mathbf{t}^{\mathrm{T}}(\tilde{\mathbf{u}}^{(1)} - \mathbf{u})\,\mathrm{d}S_1 + \oint_{c_2} \mathbf{u}^{\mathrm{T}}\tilde{\mathbf{t}}^{(2)}\,\mathrm{d}S_2 \tag{1}$$

where σ and **u** are the stress and displacement vectors in Ω, **t** is the surface traction vector, **S** is the elastic compliance matrix, and **D** is the matrix differential operator relating strains to displacements. The displacement vector $\tilde{\mathbf{u}}^{(1)}$ on c_1 and the traction vector $\tilde{\mathbf{t}}^{(2)}$ on c_2 are specified and assumed known.

The stationary value of the functional defined by (1) yields the following set of equations:

$$\mathbf{D}^{\mathrm{T}}\sigma = 0 \quad \text{in } \Omega \tag{2}$$

$$\mathbf{S}\sigma = \mathbf{D}\mathbf{u} \quad \text{in } \Omega \tag{3}$$

$$\mathbf{t} = \mathbf{n}^{(1)}\sigma \quad \text{on } C_1 \tag{4}$$

$$\mathbf{u} = \tilde{\mathbf{u}}^{(1)} \quad \text{on } C_1 \tag{5}$$

$$\sigma\mathbf{n}^{(2)} = \tilde{\mathbf{t}}^{(2)} \quad \text{on } C_2 \tag{6}$$

As indicated by Zhang[8], σ, **t**, and **u** in functional (1) can be chosen in such a manner that equations (2)–(4) are automatically satisfied. By doing this, functional (1), which involves the area integration, can be significantly reduced to the line integration of the boundary as follows:

$$\Pi_e = \frac{1}{2}\left(\oint_{c_1} \mathbf{t}^{\mathrm{T}}\mathbf{u}\,\mathrm{d}S_1 - \oint_{c_2} \mathbf{t}^{\mathrm{T}}\mathbf{u}\,\mathrm{d}S_2\right) - \oint_{c_1} \mathbf{t}^{\mathrm{T}}\tilde{\mathbf{u}}^{(1)}\,\mathrm{d}S_1 + \oint_{c_2} \mathbf{u}^{\mathrm{T}}\tilde{\mathbf{t}}^{(2)}\,\mathrm{d}S_2 \tag{7}$$

In Reference 8, the specified boundary traction $\tilde{\mathbf{t}}^{(2)}$ on c_2 are assumed to be zero. Two special approximating functions for the stress and displacement fields are constructed based on the

classical elasticity solutions for a multiply connected circular region. The two holomorphic functions in the general expressions of the elasticity solutions are expanded into two complex Laurent series. The stress and displacement fields are expressed as follows:

$$\begin{Bmatrix} \sigma_{11} \\ \sigma_{22} \\ \sigma_{12} \end{Bmatrix} = \sum_{k=m_b}^{m_u} \begin{bmatrix} 2A_1 - A_3 & -2A_2 + A_4 & -A_1 & A_2 \\ 2A_1 + A_3 & -2A_2 - A_4 & A_1 & -A_2 \\ A_4 & A_3 & A_2 & A_1 \end{bmatrix} \begin{Bmatrix} \tilde{a}_k \\ \hat{a}_k \\ \tilde{b}_k \\ \hat{b}_k \end{Bmatrix} \tag{8}$$

$$\begin{Bmatrix} u_1 \\ u_2 \end{Bmatrix} = \frac{1}{2\mu} \sum_{k=m_b}^{m_u} \begin{bmatrix} \kappa B_1 - B_3 & -\kappa B_2 + B_4 & -B_1 & B_2 \\ \kappa B_2 + B_4 & \kappa B_1 + B_3 & B_2 & B_1 \end{bmatrix} \begin{Bmatrix} \tilde{a}_k \\ \hat{a}_k \\ \tilde{b}_k \\ \hat{b}_k \end{Bmatrix} \tag{9}$$

where

$$A_1(k,r,\theta) = kr^{k-1}\cos(k-1)\theta \tag{10}$$

$$A_2(k,r,\theta) = kr^{k-1}\sin(k-1)\theta \tag{11}$$

$$A_3(k,r,\theta) = k(k-1)r^{k-1}\cos(k-3)\theta \tag{12}$$

$$A_4(k,r,\theta) = k(k-1)r^{k-1}\sin(k-3)\theta \tag{13}$$

$$B_1(k,r,\theta) = r^k\cos k\theta \tag{14}$$

$$B_2(k,r,\theta) = r^k\sin k\theta \tag{15}$$

$$B_3(k,r,\theta) = kr^k\cos(k-2)\theta \tag{16}$$

$$B_4(k,r,\theta) = kr^k\sin(k-2)\theta \tag{17}$$

The A_1 through B_4 in the matrices are functions of the integer k and the polar coordinates r and θ with the origin at the centre of the hole. μ and ν are the shear modulus and Poisson's ratio, respectively. $\kappa = (3-\nu)/(1+\nu)$ for plane stress problems, and $\kappa = 3 - 4\nu$ for plane strain problems. m_u and m_b are the upper and lower limits of the series. We can rewrite equations (8) and (9) as follows:

$$\sigma = \mathbf{P}\beta \tag{18}$$

$$\mathbf{u} = \mathbf{U}\beta \tag{19}$$

where σ and $\mathbf{u}$ are the vectors of stress and displacement components, $\sigma = [\sigma_{11}\ \sigma_{22}\ \sigma_{12}]^T$ and $\mathbf{u} = [u_1\ u_2]^T$, β is the vector of the real unknown coefficients, $\beta = [\tilde{a}_k, \hat{a}_k, \tilde{b}_k, \hat{b}_k]^T$ for $k = m_b, m_u$, and $\mathbf{P}$ and $\mathbf{U}$ are matrices relating the stresses and displacements to the unknown coefficients as in equations (8) and (9).

In this work, we will consider the case where a hole is subjected to a non-zero uniform pressure. Since the resultant force and moment along the circular boundary are zero, the same stress and

displacement expressions used in Reference 8 can be employed in our case. Using equations (4) and (8), the traction can be expressed as

$$\mathbf{t} = \mathbf{R}^{(\alpha)}\beta \quad C_\alpha, \quad \alpha = 1, 2 \tag{20}$$

where

$$\mathbf{R}^{(\alpha)} = \mathbf{n}^{(\alpha)}\mathbf{P} \tag{21}$$

and $\mathbf{n}^{(\alpha)}$ is a 2×3 matrix of outward unit normal to the boundary.

The specified displacement $\tilde{\mathbf{u}}^{(1)}$ is assumed to take the following form

$$\tilde{\mathbf{u}}^{(1)} = \mathbf{L}\mathbf{q} \tag{22}$$

where $\mathbf{L}$ is the matrix representing the displacement (linear or quadratic) interpolation function. For linear interpolation function between two nodes i and $i+1$ (shown in Figure 1), with nodal displacements (u_1^i, u_2^i) and (u_1^{i+1}, u_2^{i+1}), $\mathbf{L}$ can be expressed as

$$\mathbf{L} = \begin{bmatrix} 1-\xi & 0 & \xi & 0 \\ 0 & 1-\xi & 0 & \xi \end{bmatrix} \tag{23}$$

where $\xi = s/d$, and d is the distance between two adjacent nodes, s is a boundary co-ordinate which is measured from node i, and $\mathbf{q}$ is the vector representing nodal displacements of the special element with the following form:

$$\mathbf{q} = [u_1^i \;\; u_2^i \;\; u_1^{i+1} \;\; u_2^{i+1}]^{\mathrm{T}} \tag{24}$$

The specified traction on c_2 can be written as

$$\tilde{\mathbf{t}}^{(2)} = -\mathbf{n}^{(2)} p_{\mathrm{o}} \tag{25}$$

where p_{o} is the uniform pressure acting on the inner boundary c_2.

Substituting equations (18)–(25) into equation (7), we obtain

$$\Pi_{\mathrm{e}} = \tfrac{1}{2}\beta^{\mathrm{T}}(\mathbf{H}^1 - \mathbf{H}^2)\beta - \beta^{\mathrm{T}}\mathbf{G}\mathbf{q} + \beta^{\mathrm{T}}\mathbf{T}_0 \tag{26}$$

where

$$\mathbf{H}^1 = \frac{1}{2}\oint_{c_1} [(\mathbf{R}^{(1)})^{\mathrm{T}}\mathbf{U} + \mathbf{U}^{\mathrm{T}}\mathbf{R}^{(1)}]\,\mathrm{d}S_1$$

$$\mathbf{H}^2 = \frac{1}{2}\oint_{c_2} [(\mathbf{R}^{(2)})^{\mathrm{T}}\mathbf{U} + \mathbf{U}^{\mathrm{T}}\mathbf{R}^{(2)}]\,\mathrm{d}S_2$$

$$\mathbf{G} = \oint_{c_1} (\mathbf{R}^{(1)})^{\mathrm{T}}\mathbf{L}\,\mathrm{d}S_1$$

$$\mathbf{T}_0 = -\oint_{c_2} \mathbf{U}^{\mathrm{T}}\mathbf{n}^{(2)} p_{\mathrm{o}}\,\mathrm{d}S_2 \tag{27}$$

The stationary value of the functional Π_{e} gives

$$(\mathbf{H}^1 - \mathbf{H}^2)\beta - \mathbf{G}\mathbf{q} + \mathbf{T}_0 = 0 \tag{28}$$

This leads to the determination of the unknown coefficients β as follows:

$$\beta = (\mathbf{H}^1 - \mathbf{H}^2)^{-1}(\mathbf{G}\mathbf{q} - \mathbf{T}_0) \tag{29}$$

Substituting equation (29) into equation (26), we obtain

$$\Pi_e = -\tfrac{1}{2}\mathbf{q}^T\mathbf{K}^e\mathbf{q} + \mathbf{q}^T\mathbf{F}^e - \tfrac{1}{2}\mathbf{T}_0^T(\mathbf{H}^1 - \mathbf{H}^2)^{-1}\mathbf{T}_0 \tag{30}$$

where

$$\mathbf{K}^e = \mathbf{G}^T(\mathbf{H}^1 - \mathbf{H}^2)^{-1}\mathbf{G} \tag{31}$$

$$\mathbf{F}^e = \mathbf{G}^T(\mathbf{H}^1 - \mathbf{H}^2)^{-1}\mathbf{T}_0 \tag{32}$$

$\mathbf{K}^e$ and $\mathbf{F}^e$, respectively, represent the element stiffness matrix and load vector for the special element. The unknown coefficient vector β can be calculated from equation (29) after the element nodal displacement $\mathbf{q}$ is obtained. The local stresses and displacements inside the super element can then be calculated from equations (8) and (9) once the vector β is determined.

3. NUMERICAL EXAMPLES

In this section, three numerical examples are presented to show accuracy, efficiency, and versatility of the proposed hybrid method. In the first example, the accuracy of the proposed method is verified against the analytical solution of an infinite (large) plate with a hole subjected to an internal pressure. In the second example, a boundary value problem of a plate with four holes is analysed, and the efficiency of the proposed method is demonstrated through the reduction in number of degrees of freedom necessary to obtain the same results by the conventional 4-noded finite elements available in ABAQUS. In the third example, the versatility of the proposed method is shown by solving a boundary value problem with random distribution of pores subjected to distinct pore pressure. The first two examples are treated as plane stress problems, while the third problem is treated as a plane strain problem. The material is assumed to be linearly elastic and isotropic. Young's modulus is 1·724 GPa (250,000 psi) and Poisson's ratio is 0·285.

3.1. A square large plate with a small hole subjected to a uniform pressure

As shown in Figure 2, we consider a 101·6 mm × 101·6 mm (4 in × 4 in) plate with a circular hole of radius 5·08 mm (0·2 in) subjected to an internal pressure $P_o = 0{\cdot}6895$ Mpa (100 psi). The outer boundary of the plate is traction free. The plate is partitioned into 61 elements, including one 8-node special hybrid element with linear displacement interpolation on each side and 60 4-node elements. These 4-node elements may be either homogeneous hybrid elements with linear displacement interpolation on the boundaries or the conventional displacement-based isoparametric elements. The values of the upper and lower limit of Laurent series m_u and m_b are set to be 5 and -5 for the special element, respectively. No significant difference is observed in the results as long as these values chosen so that the resultant matrix is rank-sufficient and satisfies the stability condition. Figures 3 and 4 show the normalized stresses and displacements in cross-section A–A. The stress and displacement distributions obtained by the proposed method coincide very well with those by the analytical solution. It is important to note that the analytical

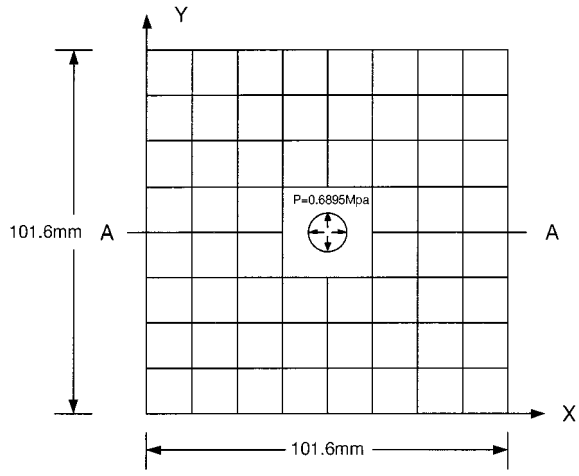

Figure 2. A large square plate with a hole (61 elements)

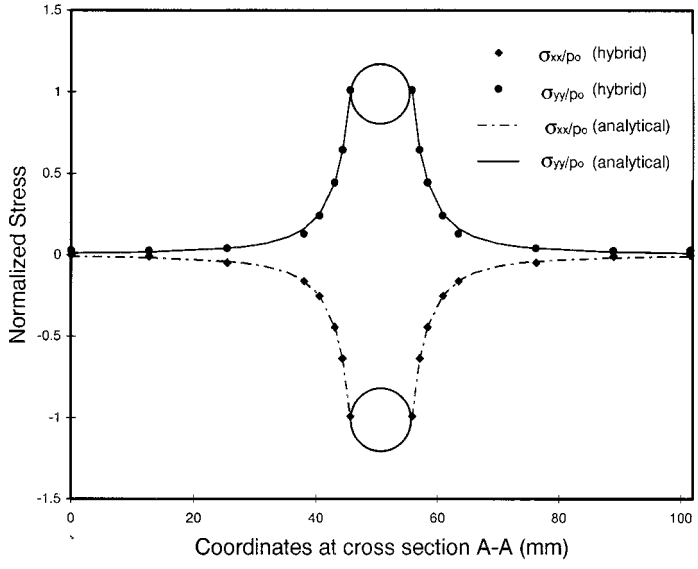

Figure 3. Normalized stresses at cross-section A–A

results are reproduced not only at the nodal points also at every point inside the special element. This demonstrates the accuracy of the developed special element for a circular hole with internal pressure.

3.2. A plate with four holes subjected to distinct internal pore pressure

As shown in Figure 5, we consider a 101·6 mm × 101·6 mm (4 in × 4 in) plate with four 5·08 mm (0·2 in) radius holes. The plate is subjected to a horizontal load 889·6N (200 lb) and a vertical load

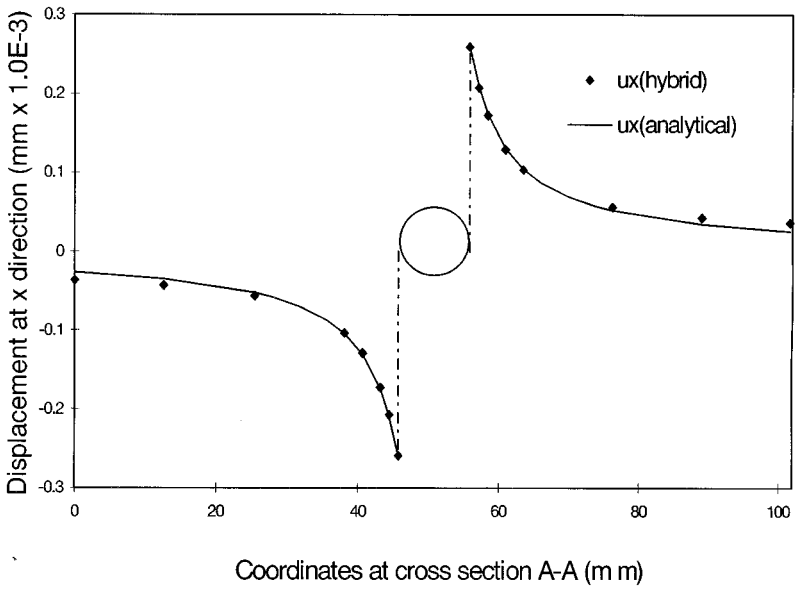

Figure 4. Displacement *ux* at cross-section A–A

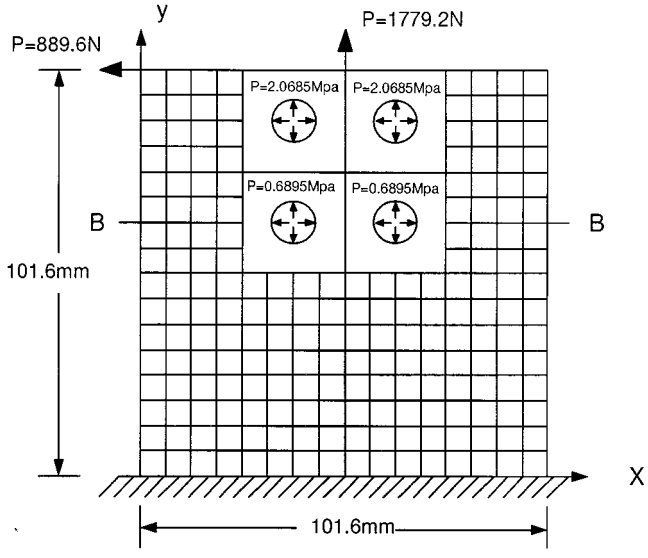

Figure 5. A square plate with 4 holes with mesh used for hybrid element analysis (196 elements)

1779·2N (400 lb) at the top end. At the bottom end, the displacement is zero. The upper two holes are subjected to internal hydrostatic pressure of 2·0685 Mpa (300 psi) while the lower two holes are subjected to 0·6895 Mpa (100 psi), respectively. The plate is partitioned into 196 elements, including 4 16-node special hybrid elements and 192 homogenous hybrid elements. Linear

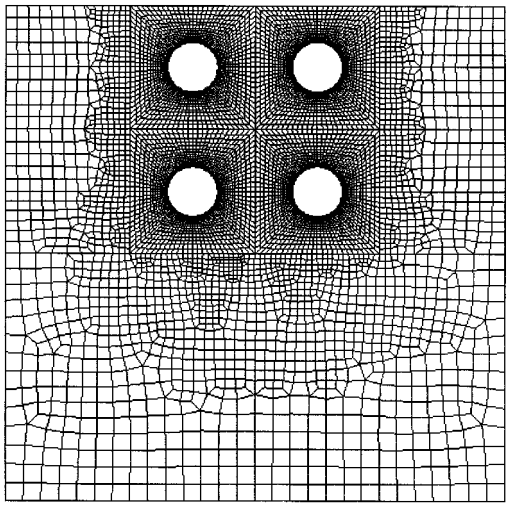

Figure 6. Conventional mesh used by ABAQUS (8832 elements, 9108 nodes)

displacement interpolation is used in each element. The same boundary value problem is analysed by ABAQUS and the corresponding mesh is shown in Figure 6. In order to get accurate results around the hole, 8892 4-node elements (9108 nodes) are used. Since the stress distribution around a hole subjected to an internal pressure is proportional to $1/r^2$ and the stress inside the traditional 4-node element assumed to be constant, a large number of elements are needed. On the contrary to the traditional method, the stress shape function inside the special element includes $1/r^2$. This leads to significant reduction in the number of elements and that of the degrees of freedom. As shown in Figures 7 and 8, the same results are obtained using the coarse mesh of 196 hybrid elements without sacrificing accuracy. The number of degrees of freedom in this example is reduced from 18,000 to 467. This clearly demonstrates the efficiency of the proposed method.

3.3. Application of the proposed method to a plate with random distribution of pores

In this example, the application of the proposed method to fluid-filled porous materials with randomly distributed pores is demonstrated. As shown in Figure 9, a 203·2 mm × 101·6 mm (8 in × 4 in) porous material (plane strain) bounded by the fixed impermeable top and bottom is subjected to fluid pressure. Seventy-nine small circular holes with distinct radii ranging from 1·778 mm (0·07 in) to 3·048 mm (0·12 in) are randomly distributed.

In reality, pores are interconnected so that a fluid flows through a porous material. In this work, a random distribution of pores with various sizes is modelled but the detailed pore-to-pore connection is omitted from the consideration. It is further assumed that the pores with different sizes are randomly distributed throughout the domain so that the permeability can be assumed to be constant in the domain and the pore pressure is assumed to be uniform within the individual pore. The fluid pressures at the right and left ends are maintained to be P_o and zero, respectively, and the fluid flow rate is constant. Since the steady-state problem is considered, the deformation

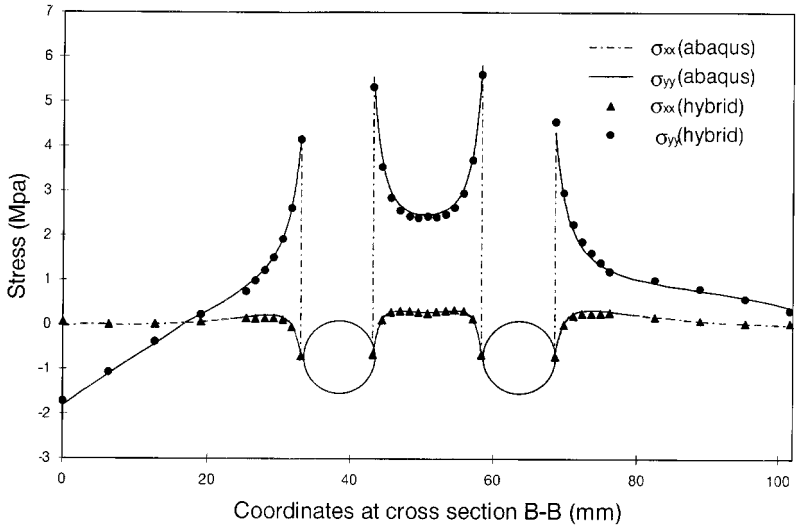

Figure 7. Normal stress components at cross-section B–B

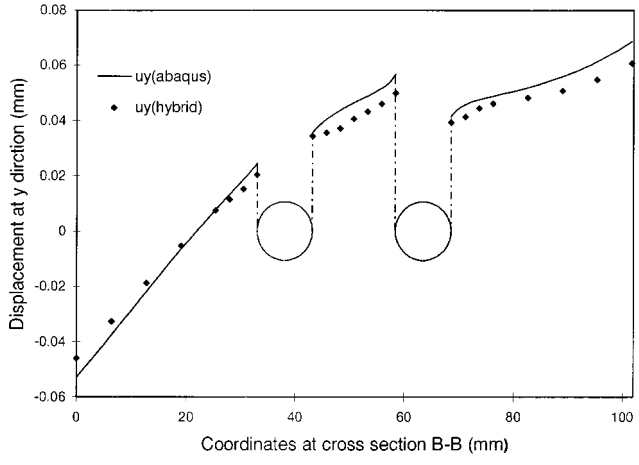

Figure 8. Displacement at cross-section B–B

of a porous material and the flow of a fluid through a porous material are uncoupled. From the Darcy's law and the fluid mass continuity, the fluid pressure is assumed to be linearly varying as a function of the x co-ordinate.

The mesh consists of 64 4-sided and 15 5-sided hybrid special elements. Doubly linear displacement interpolation is used along all element boundaries. The values of m_u and m_b are chosen to be 5 and -5 for the 4-sided elements and 6 and -6 for the 5-sided ones. Figure 10 shows the normal stress $\sigma_{\theta\theta}$ along the pore boundary of pore #A in Figure 9. The local stresses are largely influenced by the position of the pores. At position angles where other pores are closely located (approximately $\theta = 100^\circ$, 240°), large stress concentrations are observed.

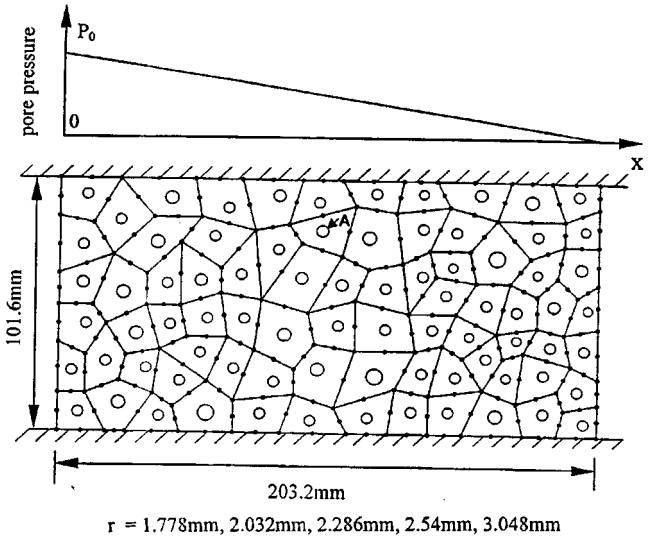

Figure 9. A fluid-filled porous material (plane strain) With 79 randomly distributed pores (64 4-sides and 15 5-sided element)

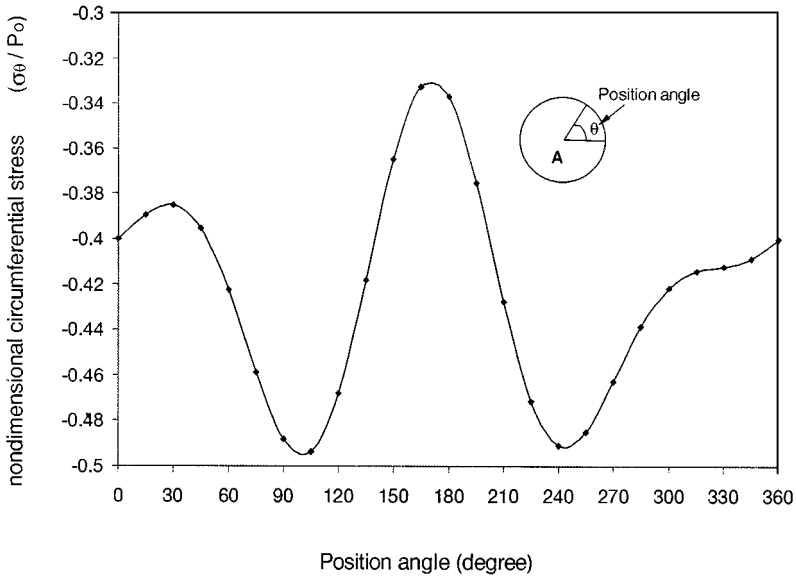

Figure 10. Normalized stress $\sigma_{\theta\theta}$ around pore #A

4. APPLICATION OF THE PROPOSED METHOD TO THERMO-ELASTIC PROBLEMS

The proposed method can be easily applied to calculation of thermal residual stress for a plane with randomly distributed pores. The governing equations for thermo-elastic plane problems

without body force are summarized as follows:

$$\sigma_{ij,j} = 0 \quad \text{in } \Omega \tag{33}$$

$$\varepsilon_{ij} = \tfrac{1}{2}(u_{i,j} + u_{j,i}) \quad \text{in } \Omega \tag{34}$$

$$\sigma_{ij} = \lambda \varepsilon_{kk} \delta_{ij} + 2G\varepsilon_{ij} - q\delta_{ij} \quad \text{in } \Omega \tag{35}$$

$$t_i = \tilde{t}_i \quad \text{in } S_\sigma \tag{36}$$

$$u_i = \tilde{u}_i \quad \text{on } S_\mathrm{u} \tag{37}$$

$$q = \frac{E\alpha\Delta T}{1 - v} \tag{38}$$

where ε_{ij} and ΔT are the strain components and temperature change, respectively. Ω is the domain we study. S_σ and S_u are the prescribed traction and displacement boundary, respectively. λ, G, E, v and α, respectively, are the Lamé constant, shear modulus, Young's Modulus, Poisson's ratio and thermal expansion coefficient.

Based on the Duhamel–Newmann analogy,[11] the thermal residual stresses can be calculated from a corresponding isothermal boundary value problem with equivalent body force and surface traction on the boundary as follows:

$$\sigma_{ij} = \sigma'_{ij} - q\delta_{ij} \tag{39}$$

where σ'_{ij} represents the corresponding isothermal stress and satisfies

$$\sigma'_{ij,j} + F_i = 0 \quad \text{in } \Omega \tag{40}$$

$$\sigma'_{ij} = \lambda \varepsilon_{kk} \delta_{ij} + 2G\varepsilon_{ij} \quad \text{in } \Omega \tag{41}$$

$$\varepsilon_{ij} = \tfrac{1}{2}(u_{i,j} + u_{j,i}) \quad \text{in } \Omega \tag{42}$$

$$F_i = \frac{E\alpha}{1 - v_i} (\Delta T)_i \quad \text{in } \Omega \tag{43}$$

$$t_i = \tilde{t}_i + qn_i \quad \text{on } S_\sigma \tag{44}$$

$$u_i = \tilde{u}_i \quad \text{on } S_\mathrm{u} \tag{45}$$

Upon solving the corresponding isothermal boundary value problem and determining σ'_{ij}, σ_{ij} can be evaluated from equation (39). When the temperature changes uniformly, the equivalent body force is zero, and the formulation discussed in Section 2 can be immediately applied to problems of calculating thermal residual stresses.

In order to show this, let us consider the plate with four holes used in Example 2 as shown in Figure 11. In this example, the displacement components of the outer boundary are zero, and the inner pore boundary is stress free. The thermal residual stress will be evaluated when the plate is subjected to uniform temperature decrease 1000°C. The Young's modulus and Poisson's ratio are the same as before, and the thermal coefficient α is 1·0E−6 (1/°C).

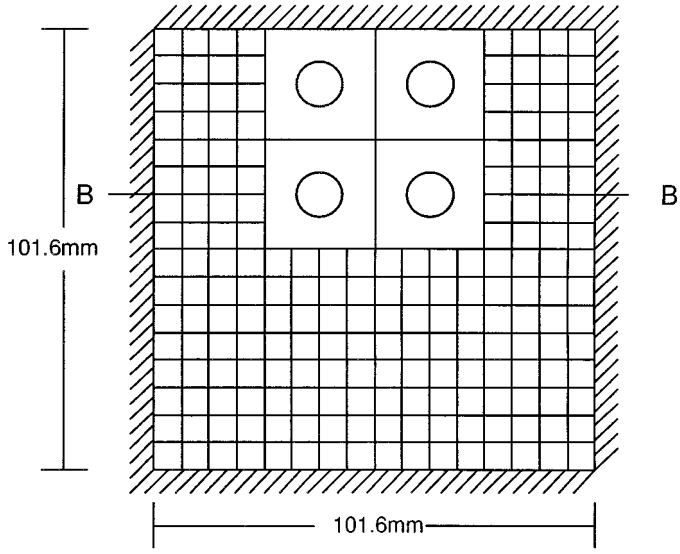

Figure 11. A square plate with 4 holes (thermal residual stress calculation due to $\Delta T = -1000°C$)

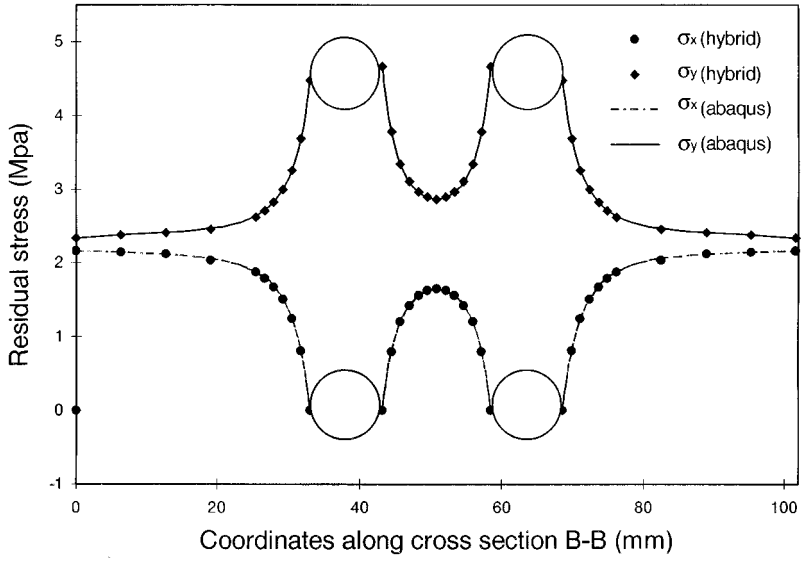

Figure 12. Thermal residual stress at cross-section B–B ($\Delta T = -1000°C$)

The temperature change is replaced by the corresponding uniform hydrostatic pressure p_o ($-2{\cdot}411$ Mpa) acting on the holes. Upon solving the corresponding isothermal boundary value problem, the thermal residual stress distribution is calculated. In Figure 12, the results obtained by the proposed method are compared with those by the traditional thermal stress analysis using

ABAQUS. Both results match very well, and the thermal residual stress components are observed to be large along the inner holes.

5. CONCLUSIONS

A hybrid finite element method is developed for fluid-filled porous materials where pores are randomly distributed and each pore is subjected to distinct hydrostatic pressure. Arbitrary n-sided polygonal elements based on the Hellinger–Reissner principle are used to mesh the heterogeneous domain. The shape functions and hybrid functional used in Reference 8 are employed, and the appropriate stiffness matrix and loading vector corresponding to the constant hydrostatic pore pressure is derived. Accuracy of the proposed method is verified by a simple analytical solution of a hole subjected to hydrostatic pressure in an infinite (large) plate. Excellent agreement is obtained. Efficiency of the proposed method is demonstrated through a boundary value problem with four holes by comparing the solutions by the developed methods with those obtained by the conventional finite element method (ABAQUS). The number of elements required to solve the same problem has been reduced from almost 9000 elements in the traditional methods to less than 200 in the proposed method. The proposed method is applied to a steady-state boundary value problem, where the fluid flow and solid deformation are uncoupled and the hydrostatic pore pressure is determined from Darcy's law and fluid mass continuity equation. The constant hydrostatic pore pressure is specified at each pore boundary, and the effect of pore distribution on local stress concentration is evaluated. Due to the analogy between the purely mechanical theory for fluid-filled porous materials and the thermo-elastic theory for porous materials, the proposed method can be also used to solve thermal residual stress due to uniform temperature change. The solution of a boundary value problem by the proposed method is verified against that based on ABAQUS.

ACKNOWLEDGEMENTS

This work was supported by the National Science Foundation under the grant No. CMS9634870.

REFERENCES

1. R. M. Christenson and K. H. Lo, 'Solutions for effective shear properties in three phase sphere and cylinder models', *J. Mech. Phys. Solids*, **27**(4), 315–330 (1979).
2. N. Pan, 'The elastic constants of randomly oriented fiber composites: a new approach to prediction', *Sci. Engng. Compos. Mater.*, **5**(2), 64–72 (1996).
3. J. Zhang and N. Katsube, 'A hybrid finite element method for heterogeneous materials with randomly dispersed rigid inclusions', *Int. J. Numer. Meth. Engng.*, **38,** 1635–1653 (1995).
4. J. Zhang and N. Katsube, 'A hybrid finite element method for heterogeneous materials with randomly dispersed elastic inclusions', *Finite Elements Anal. Des.*, **19**(1), 45–55 (1995).
5. J. Zhang and N. Katsube, 'A polygonal element approach to random heterogeneous media with rigid ellipses or elliptical voids', *Comput. Meth. Appl. Mech. Engng.*, **148,** 225–234 (1997).
6. S. Ghosh and S. N. Mukhopadhyay, 'Microstructure-based finite element analysis of heterogeneous media involving Dirichlet tessellations', *Comput. Meth. Appl. Mech. Engng.*, **104,** 211–247 (1993).
7. S. Moorthy and S. Ghosh, 'Model for analysis of arbitrary composite and porous microstructures with Voronoi cell finite elements', *Int. J. Numer. Meth. Engng.*, **39,** 2363–2398 (1996).
8. J. Zhang, 'A hybrid finite element method for heterogeneous media with random microstructures', *Ph.D. Dissertation*, The Ohio State University, 1995.
9. P. Tong, T. H. H. Pian and S. J. Lasry, 'A hybrid-element approach to crack problems in plane elasticity', *Int. J. Numer. Meth. Engng.*, **7,** 297–308 (1993).
10. R. Piltner, 'Special finite elements with holes and internal cracks', *Int. J. Numer. Meth. Engng.*, **21,** 1471–1485 (1985).
11. Y. C. Fung, *Foundations of Solid Mechanics*, Prentice-Hall, Englewood Cliffs, NJ, 1965.

